

Alternating current flashover voltage of a uniform polluted glass flat insulator under parallel electric discharges effect

Samia Satta¹, Abdelhafid Bayadi², Rabah Boudissa³

¹Research Center of Industrial Technologies, Algiers, Algeria

²Department of Electrotechnic, Faculty of Technology, University Ferhat Abbas Setif 1, Sétif, Algérie

³Laboratory Electrical Engineering, Faculty of Technology, University Abderrahmane Mira, Béjaia, Algérie

Article Info

Article history:

Received Apr 26, 2021

Revised Feb 15, 2022

Accepted Mar 8, 2022

Keywords:

Alternative voltage

Effective discharge length

Flashover

Glass laboratory insulator model

Pollution degree

Uniform pollution

ABSTRACT

This work presents a study aiming to analyze the development of parallel discharges on insulating surfaces of different sizes uniformly polluted. Moreover, it is aimed to find an equivalence between multiple point-point and plane-plane configurations. The study is carried out under alternating current (AC) voltage. The effects of many parameters on the electric strength of the considered air gap system configurations are presented. These parameters are the length of the creepage distance, the pollution degree and the contaminated surface width. Glass rectangular surface are used for the tests. Finally, a video camera system is used to support this investigation by laboratory observations of the full process of flashover mechanism. The obtained results show that there is a width limit approximately equal to 8 cm beyond which several arcs, parallel, consecutive and independent can develop. This limit represents the minimal electrical performance of the insulation and we did not observe any effect of the volume conductivity on it.

This is an open access article under the [CC BY-SA](https://creativecommons.org/licenses/by-sa/4.0/) license.



Corresponding Author:

Abdelhafid Bayadi

Department of Electrical Engineering, Faculty of Technology, University Ferhat ABBAS Setif 1

Cité Maabouda, Route de Béjaia, 19000, Algeria

Email: a_bayadi@univ-setif.dz

1. INTRODUCTION

Outdoor high voltage insulation constitutes a crucial element for the design and performance of large high voltage power systems. Due to the critical importance of a reliable and efficient power transmission, outdoor insulation has inevitably been at the epicenter of research interest in an endeavor to eliminate or alleviate the problems associated with insulation failure [1]. Interruptions or just failures within the power systems may result not only in damage to valuable high-voltage equipment, but can also lead to considerable loss of revenue, particularly for industrial consumers. While in use, line insulators must withstand a wide range of voltage magnitude under normal operating conditions, as well as surge transients imposed by lightning strikes and switching operations. Ceramic insulation systems, such as glass and porcelain insulators, have been in use for more than 100 years [2]. Ceramic insulators have demonstrated a proven track record in various aspects of the insulation performance, particularly ageing and lifespan. In addition to high mechanical strength, they provide excellent resistance to material degradation cause by electrical stress and discharge activities [3]. However, pollution and humidity strongly affect their electrical performance [4].

In practice, outdoor insulators are constantly exposed to various environmental contaminants, including natural and agricultural substances and industrial emissions, during their period of service. The contaminants may form a conducting or partially conducting surface layer when exposed to wet atmospheric conditions such as fog, mist and drizzle. The presence of pollutants covering the insulator surface could also

promote the formation of a continuous conductive film. The resulting leakage current under system voltage generates heating that evaporates water from the wet surfaces, risking the formation of dry bands [5]. In polluted environments with high moisture levels, electrical discharges will develop on the insulator surfaces, coupled with the high electric field, trigger electrical discharges. In favorable conditions, the discharges may elongate over many dry bands and, consequently, may lead to complete flashover [6].

Published studies of the pollution behavior of insulators of various forms under direct current (DC), alternating current (AC) and impulse voltage from the theoretical [7]–[10] or experimental [11]–[18] point of view helped in improving the knowledge of their performance under pollution conditions. These researchers have shown the non-uniformity of the pollution distribution on insulators surface in real service conditions. In other words, the observations made on the transmission lines show that the quantity of pollution deposited on the upper face of the insulator is different from that deposited on the lower face. Furthermore, it has been observed that the distribution of the pollution along the axial and radial direction of the insulators string is non-uniform. This situation is attributed to several factors, among which we can cite (the shape and surface condition of the insulator, the type of pollution, the role of rain and wind). The pollution performance investigations conducted by different researchers have shown that the flashover of insulators is affected by various parameters [18]–[25] acting simultaneously.

The perimeter of the insulator is considered to be one of the dominant factors involved in the development of discharges on its surface. That is, in the case of small diameter insulator the flashover occurs just after the formation and the propagation of a discharge on its surface. However, for the large insulators when contaminated uniformly, several parallel partial arcs can be observed [1], [11], [12], [14]. These arcs can grow and may develop to a full flashover. Therefore, this parameter will dictate the insulator flashover performance.

In work [20], when the authors worked on the quantification of the effect of pollution distribution on insulators flashover under AC voltage, it was noted that for thin and uniformly polluted insulator the flashover can be described by a circuit equivalent to only one electric arc connected in series with a resistance of the pollution layer. On the other hand, if the diameter of the insulators is large, a certain number of parallel partial arcs can arise simultaneously on their uniformly polluted surface and can amplify to give a complete flashover. The flashover voltage and the number of parallel arcs depend on this parameter. In the same time, it was proved that a limit characterizing the effective width corresponds to the minimum distance between two consecutive parallel critical arcs in the independent development phase. In this case, each arc has the same probability to extend in a flashover arc of the polluted surface.

Bouchelga and Boudissa [26] have carried out a research to study the impact of the parallel electric discharges' development on the insulation's performance under DC voltage. They confirmed the existence of a limit distance between two consecutive electric arcs which is approximately 12 cm in positive polarity and 20 cm in negative polarity. It was, also, noted that this limit is not influenced at all by the variation of the wet layer's volume conductivity. In addition [22], the results indicate that any plane-plane system of electrodes can be associated with multiple rods-rods configurations, which have the same performance.

This paper, in continuation with the previous researches on the electrical characteristics of polluted insulator, presents findings of experiments which allow quantifying the effects of the pollution on glass insulation, the degree of its contamination and the electrodes system configurations (plane-plane and multiple rods) on the development of the parallel and independent discharges until the full flashover of the insulator when an AC voltage is applied. The results of this experimental investigation are described in this paper and the main parameter considered is the flashover voltage.

2. EXPERIMENTAL SETUP AND TEST PROCEDURE

The experimental model, illustrated in Figure 1, is composed of three different electrodes system arrangements. The first one is a plane-plane electrodes system as shown in Figure 1(a). The second is a rod-plane system as shown in Figure 1(b) and the last one is a multi-rod-rod electrodes system as shown in Figure 1(c). In all these test cells systems, the electrodes are made up of iron. The electrodes rod is cylindrical, having a diameter of about 7.5 mm and a length of 25 cm, terminated by a conical point having an angle of 60° and a radius of curvature equal to 0.4 mm. The electrode is fixed on one of the holes along the Polyvinyl chloride (PVC) tube having 40 cm in length and 4 cm in diameter as shown in Figure 1. The plane electrodes have the shape of a half cylinder of 4 cm diameter and are of different lengths. The inter-electrodes distance (L_f) is kept constant during all the tests and is equal to 10 cm. In the case of the multi rod-rod electrodes system the distance separating two adjacent rods (l_{pp}) varies according to the number of rods deposited on both sides of the insulation's surface.

The insulating specimens are made of 5 mm thick glass and are of rectangular shape, the dimensions of which are 20×32 cm. The characterization of the flat insulator performance and the visualization of the

electric phenomenon evolving in the air gap was carried out according to the electrical diagram illustrated in Figure 2 and Table 1.

A suspension is prepared using the following composition consisting of: distilled or tap water, 20 g of kaolin per liter and a suitable amount of Sodium chloride of commercial purity. The desired volume conductivity is reached by adjusting the amount of salt in the solution. The obtained electrical conductivity of the prepared solution was measured and found between 17 $\mu\text{S}/\text{cm}$ and 10 mS/cm . The choice is done to reproduce the unfavorable conditions prevailing in the real life. The application of the pollution layer on the hydrophilic sample is carried out according to the international standards. The polluted bandwidth is varied between 4 cm and 32 cm. Before each new test, the sample of desired size is cleaned and rinsed then dried.

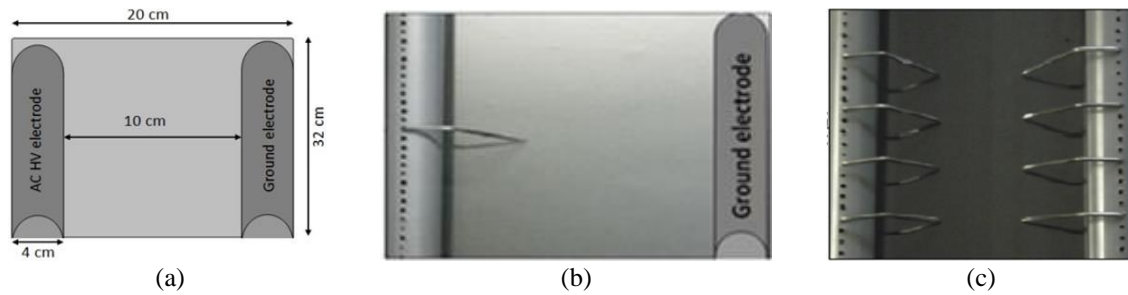


Figure 1. View of the studied configurations; (a) plane-plane, (b) rod-plane, and (c) multiple rods-rods

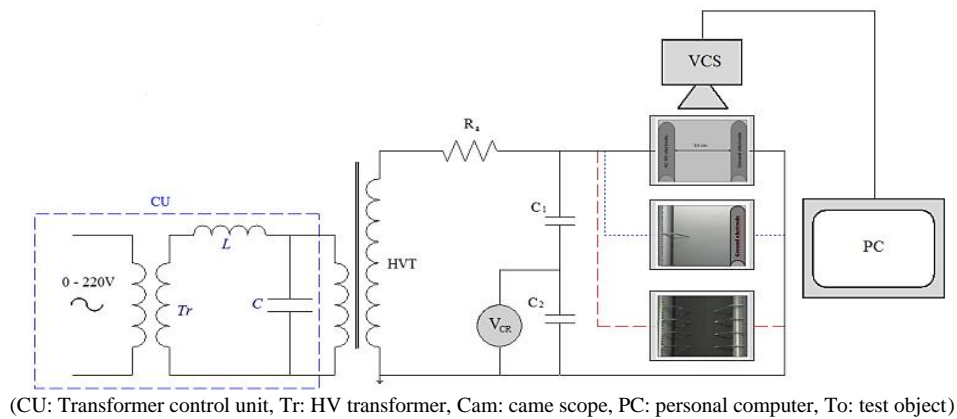


Figure 2. Laboratory test setup

Table 1. Glass characteristics

Characteristics	Value
Dielectric strength	50 à 100 kV/mm and 0.5 To 1 kV/mm à 400 °C
Relative permittivity	5 à 8
Resistivity at 20 °C	10^{10} à $10^{16} \Omega \text{ cm}$

The AC test circuit, used in this study in Figure 2, consists of a 135 kV; 8 kVA HV transformer (Tr) connected to the autotransformer integrated in SG and which allows the voltage to be adjusted to the desired value. A maximum allowed secondary voltage is 135 kV. A control unit (CU) for adjusting the speed ramp. A peak voltmeter (V_{CR}) across the low voltage arm of the capacitive divider (C_1 , C_2) to measure the flashover voltage. A protection resistance (R_a) of about 106 $\text{k}\Omega$ was connected in series with test object (To). A video camera system was then used to visualize and record the development of the electrical discharge along the sample surface from inception to full flashover.

In order to prevent the sample from drying out, the test is carried out immediately after the application of the pollution on it. It is emphasized here that 25 disruptive tests were carried out for each degree of pollution severity. The voltage is increased at a rate of 4 kV/s until the complete breakdown is obtained. The breakdown voltage is taken equal to the mean value calculated for each series of tests. During

the laboratory tests, the maximum dispersion affecting the measurement of the flashover voltage between each value of the 25 tests and the average value is kept within 5% margin. Moreover, the disruptive discharge voltage measured in given test conditions (temperature (T), pressure (P), humidity (H)) is converted to the equivalent value under the standard reference atmospheric conditions ($T_0=20\text{ }^\circ\text{C}$, $P_0=101.3\text{ kPa}$, $H_0=11\text{ g/m}^3$).

3. RESULTS AND DISCUSSION

It has been observed both from service experience and laboratory tests that the contamination flashover voltage is then strongly dependent upon the diameter, irrespective of the profile. For a given contamination severity, it might be thought that flashover voltage would decrease indefinitely with increasing diameter of insulator because the overall resistance, which limits the arc current, would also decrease similarly and hence the Lf required for any profile has to be increased. However, an increase in diameter does not reduce the flashover voltage correspondingly. This may be due to the fact that more than one arc can initiate across a single dry band, causing a higher electrode voltage drop that partially compensates for the decrease in the flashover voltage.

3.1. Pollution flashover voltage process

Figure 3 shows the different flashover stages of a flat insulator with uniform pollution and surface conductivity equal to $\sigma_{v1} = 10\text{ mS/cm}$. In this case, a plane-plane electrode system is used. The pollution flashover process can be described essentially as follows: i) firstly, many parallel arcs take place simultaneously at the high-voltage and ground electrodes, on polluted area of the insulator in Figure 3(a); ii) in the second phase, after a certain delay of time, the multiple parallel partial arcs emanating from the electrodes elongate towards each other and become longer in Figure 3(b). In this case, each of them can be transformed into arc; iii) then, these discharges progress in such a way that their number diminishes with their elongation. The small arcs extinguish to feed some discharges that may be considered as main arcs. These later become thicker and gain more energy each time the electric field increases in Figure 3(c); iv) in this stage, the main discharges progress again and occupy increasing lengths in Figure 3(d); and v) finally, As soon as they reach their critical length, their number reduces to a single discharge and a full flashover of the polluted area of the insulator is observed in Figure 3(e).

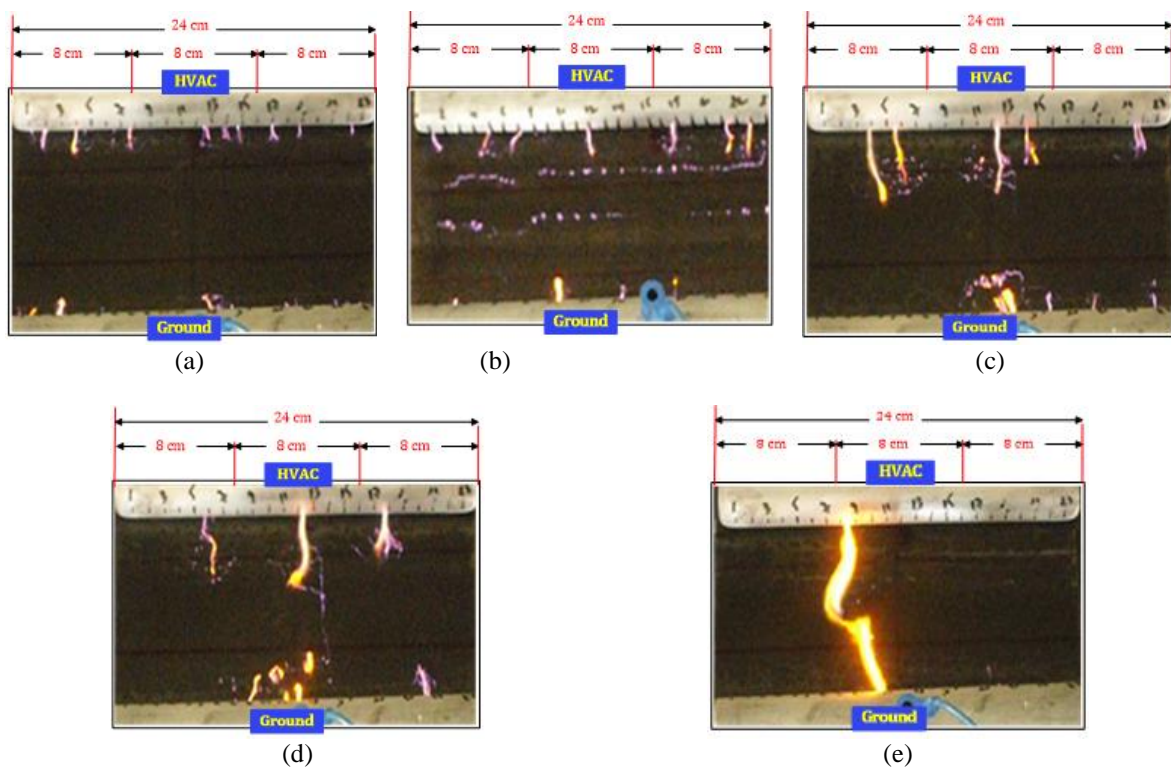


Figure 3. Pollution flashover process in (a) birth of partial parallel arcs, (b) elongation of arcs, (c) feeding of some discharges, (d) main discharges progress, and (e) full flashover

3.2. Polluted width effect on the flashover voltage

Figures 4(a) to 4(c) illustrate the relationship between the contamination flashover voltage and polluted width L_p for a conductivity equal to 0.0017, 1 and 10 mS/cm respectively using a rod-rod electrode system configuration. As mentioned previously, for each degree of pollution severity, 25 disruptive tests were carried out. The selected breakdown voltage is the average value calculated for each series of tests in Figures 4(a) to 4(c), red graph). During the laboratory tests, the maximum dispersion (discrepancies) affecting the measurement of the flashover voltage between each value of the 25 tests and the average value is within 5% margin. Moreover, for each calculated mean value, by applying correction factors, a disruptive discharge voltage measured in given test conditions (temperature T, pressure P, humidity H) is converted to the equivalent value under the standard reference atmospheric conditions ($T_0 = 20\text{ }^\circ\text{C}$, $P_0 = 101.3\text{ kPa}$, $H_0 = 11\text{ g/m}^3$) as recommended by existing international standards Figures 4(a) to (c), blue graph.

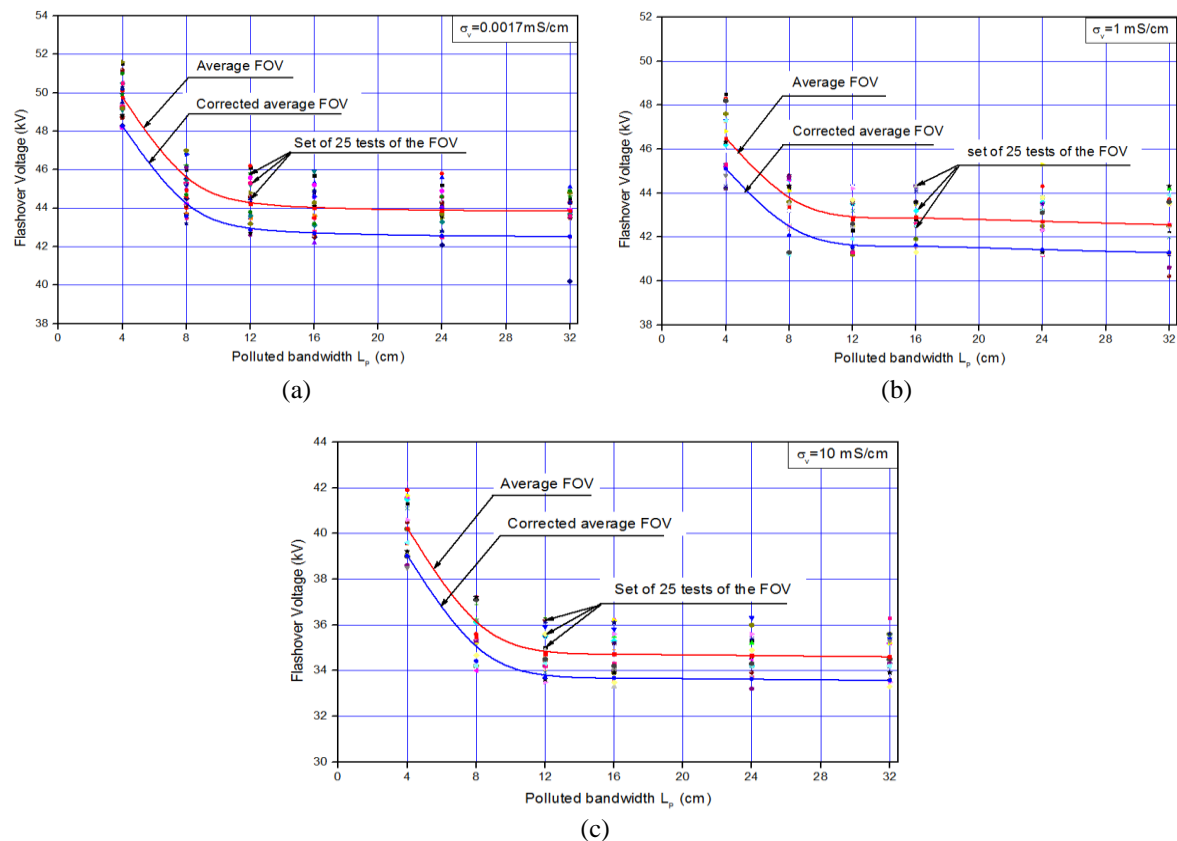


Figure 4. Variation of the FOV for the 25 tests (for $\sigma_v=10\text{ mS/cm}$); (a) $\sigma_v=0.0017\text{ mS/cm}$, (b) $\sigma_v=1\text{ mS/cm}$, and (c) $\sigma_v=10\text{ mS/cm}$

3.3. Solution conductivity effect on the flashover voltage

As mentioned before, the work focus on the behavior of parallel discharges developed on the polluted plane model during the flashover process and on the critical discharge width just before the insulator flashover. A uniformly deposited layer with different conductivities and widths covers the insulator. In the same time, obtaining an equivalence between multi rods-rods and plane-plane configurations. To understand clearly the flashover mechanism from the beginning of the discharge phenomena until the final electric arc it is necessary to consider both the important parameters namely the bandwidth and the number of parallel discharges. To this end, we have chosen two conductivity values of the pollution solution. The first is taken as $\sigma_{v1} = 17\text{ }\mu\text{S/cm}$ and the second is equal to $\sigma_{v2} = 10\text{ mS/cm}$. The length of the creepage distance is kept constant and is equal to $L_f = 10\text{ cm}$ for the 3 configurations studied. Figure 5 shows sketch of the experimental procedure followed in this first investigation. Indeed, the distance separating two successive electrodes is varied manually by shifting each of the electrodes from one position to another according to the desired distance.

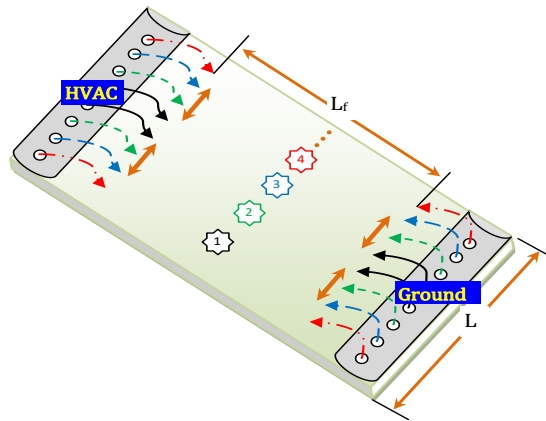


Figure 5. Distance between two successive electrodes

The distance between the two holes is equal to 1 cm. The pollution layer is deposited on the whole sample on which the tests will be performed. It should be noted that increasing the polluted bandwidth limits the number of rods that can be used for a given plate. The study was carried out on two plates whose dimensions are 20×24 cm designated as sample "A" and 20×32 cm designated as sample "B". In this first investigation, an electrodes system consisting of four electrodes is used. The AC tests were performed using the test setup discussed before to determine the flashover voltage over the polluted bandwidth range for the used conductivities and the results are plotted in Figure 6(a).

As can be seen in this figure, the overall shape of the four curves is similar. Within the region from low bandwidth up to the allowed maximum bandwidth (6 cm for the sample "A" and 8 cm for sample "B") the measured flashover voltage falls rapidly. This trend is also observed when the number of rods in the test cell is reduced to three in Figure 6(b) with the difference that in the bandwidth range from 8 cm to 10 cm, there is an indication of a relatively flat region for the case of sample "B" that is not very clear. The flattening out which, in fact, occurred on sample "B" does not exist at all on sample "A". This is because of the limitation in its dimensions. The construction of the empirical equation binding the size of the critical arc and the number of dry zones in series that are short-circuited by this arc to its effective width is based on that established in alternating voltage by Erler [11] and the two preceding methods. This can be formulated as (1):

$$L_{eff} = \frac{3}{n} Lc \tag{1}$$

with:

L_{eff} : distance between two consecutive parallel arcs (cm);

Lc : critical length of the arc (cm);

n : number of dry zones series-connected;

The empirical equation found by Erler [11] has as a relation:

$$L_{eff} = \frac{3}{n} Lc = \frac{3 Lf}{2n} \tag{2}$$

where:

$$Lc = \frac{Lf}{2} \tag{3}$$

with:

Lf : creepage distance of the insulation (cm);

As can be seen in this figure, the overall shape of the four curves is similar. Within the region from low bandwidth up to the allowed maximum bandwidth (6 cm for the sample "A" and 8 cm for sample "B") the measured flashover voltage falls rapidly. This trend is also observed when the number of rods in the test cell is reduced to three in Figure 6(b) with the difference that in the bandwidth range from 8 cm to 10 cm, there is an indication of a relatively flat region for the case of sample "B" that is not very clear. The flattening out which, in fact, occurred on sample "B" does not exist at all on sample "A". This is because of the limitation in its dimensions. A similar picture is obtained with an electrodes system consisting of only two

electrodes. The measured results are plotted in Figure 6(c). As can be seen from the figure, there is a trend of decreasing the field-of-view (FOV) with the polluted bandwidth from 1cm up to a limit of 8 cm.

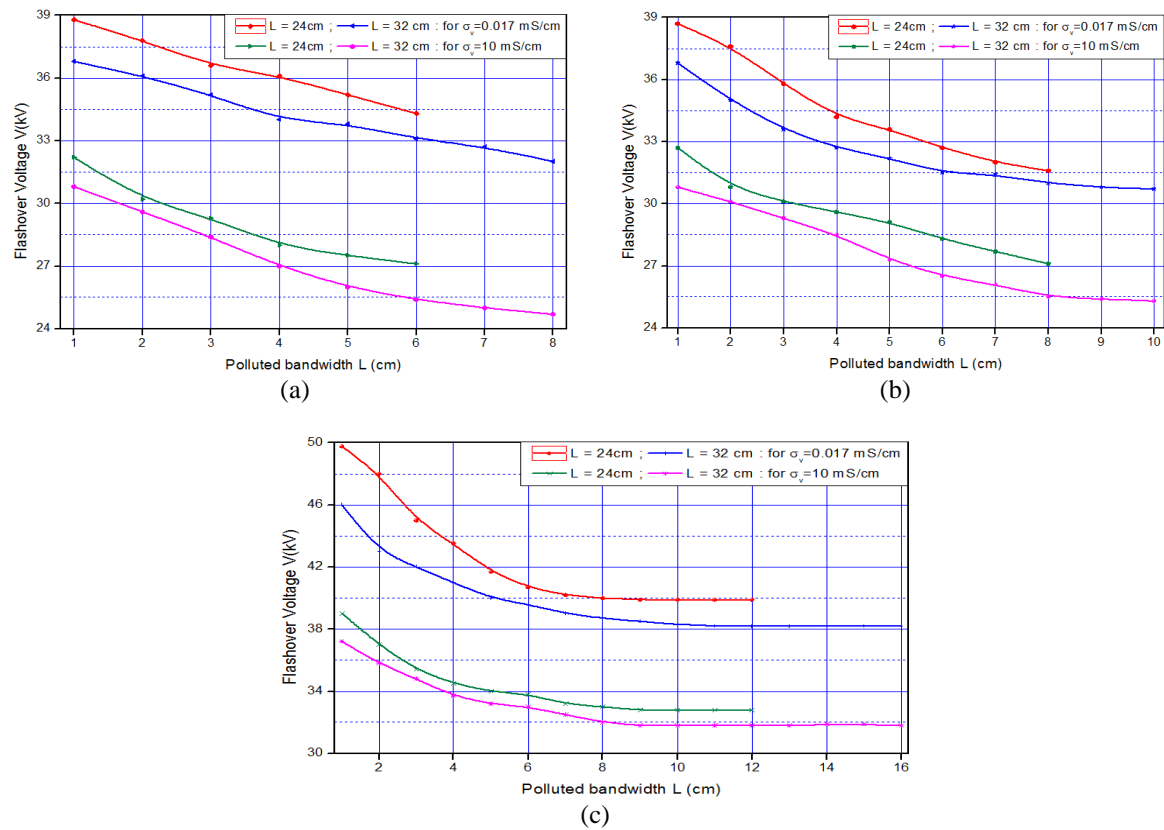


Figure 6. Effect of polluted bandwidth L_p on the flashover voltage for various configurations and conductivities: (a) case of four electrodes system and (b) case of three electrodes system, and (c) case of two electrodes system

However, increasing the polluted width beyond this limit up to 16 cm does not result in significant flashover voltage change and the shape of the curves shows a relatively flat region in this range. In (1) can be used to determine the percentage change in the measured flashover voltage when the distance between two successive electrodes is varied from 1 cm to 16 cm.

$$\delta V_{FOV} \% = \frac{V_i - V_{i+1}}{V_i} \cdot 100, \quad i = 1, k \tag{4}$$

where V_i is the i th average measured flashover voltage.

The calculated results are summarized in Table 2. As can be seen from the table, the percentage change in the flashover voltage is significant in the range of L_p between 1 cm and 8 cm. However, this change is very small or even null and then can be ignored when L_p exceeds 8 cm. The results of these calculations confirmed the previous findings concerning the observed trend of the flashover voltage.

As an example, the obtained views of the dry band sizes taken at the end of one of the tests for two samples are shown in Figure 7. These samples were in Figure 7(a) 20×8 cm in which only one electrode system is used, in Figure 7(b) 20×16 cm where again only one electrode system is used and in Figure 7(c) 20×16 cm where a 2 rods to 2 rods system is used. As can be seen from the image a good agreement has been obtained between the dry band sizes and the minimum distance between two consecutive parallel critical arcs in the independent development phase. From this first investigation, it can be concluded that a polluted bandwidth equal to 8 cm is referred to as the “effective width” beyond which no noticeable effect on the value of the flashover voltage was found. In the same time this quantity corresponds to the minimum distance between two consecutive multiple parallel arcing that takes place in the independent development phase.

Table 2. Percentage change in the flashover voltage with distance between two successive electrodes "L_p" from 1-16 cm

Number of electrodes	L _p cm	σ _v L mS/cm cm	L (cm)														
			2	3	4	5	6	7	8	9	10	11	12	13	14	15	16
4 / 4	0.017	24 --	5.38	1.64	1.39	2.56	2.62										
		32 --	1.90	2.49	3.69	0.29	2.07	1.21	2.14								
	10	24 --	6.21	2.98	4.44	1.79	1.45										
		32 --	3.90	4.05	3.17	2.55	5.22	1.57	1.20								
3 / 3	0.017	24 --	2.84	4.79	4.47	1.75	2.68	2.14	1.25								
		32 --	4.89	4.00	2.68	1.53	2.17	0.32	1.27	0.65	0.32						
	10	24 --	5.81	2.27	1.66	1.69	2.75	2.12	2.17								
		32 --	2.27	2.66	2.05	4.88	2.93	1.51	2.30	0.39	1.57						
2 / 2	0.017	24 --	4.00	6.25	3.33	4.14	2.64	0.99	0.50	0.50	0.50	0.51	0.00				
		32 --	6.52	2.33	1.67	3.15	0.50	2.01	0.77	0.52	1.30	0.00	0.00	0.00	0.00	0.00	0.00
	10	24 --	5.13	4.32	3.39	0.58	0.59	1.78	0.60	0.61	0.00	0.61	0.00				
		32 --	3.76	2.79	2.87	1.78	0.30	1.81	1.54	0.62	0.63	1.27	0.64	0.00	0.00	0.00	0.00

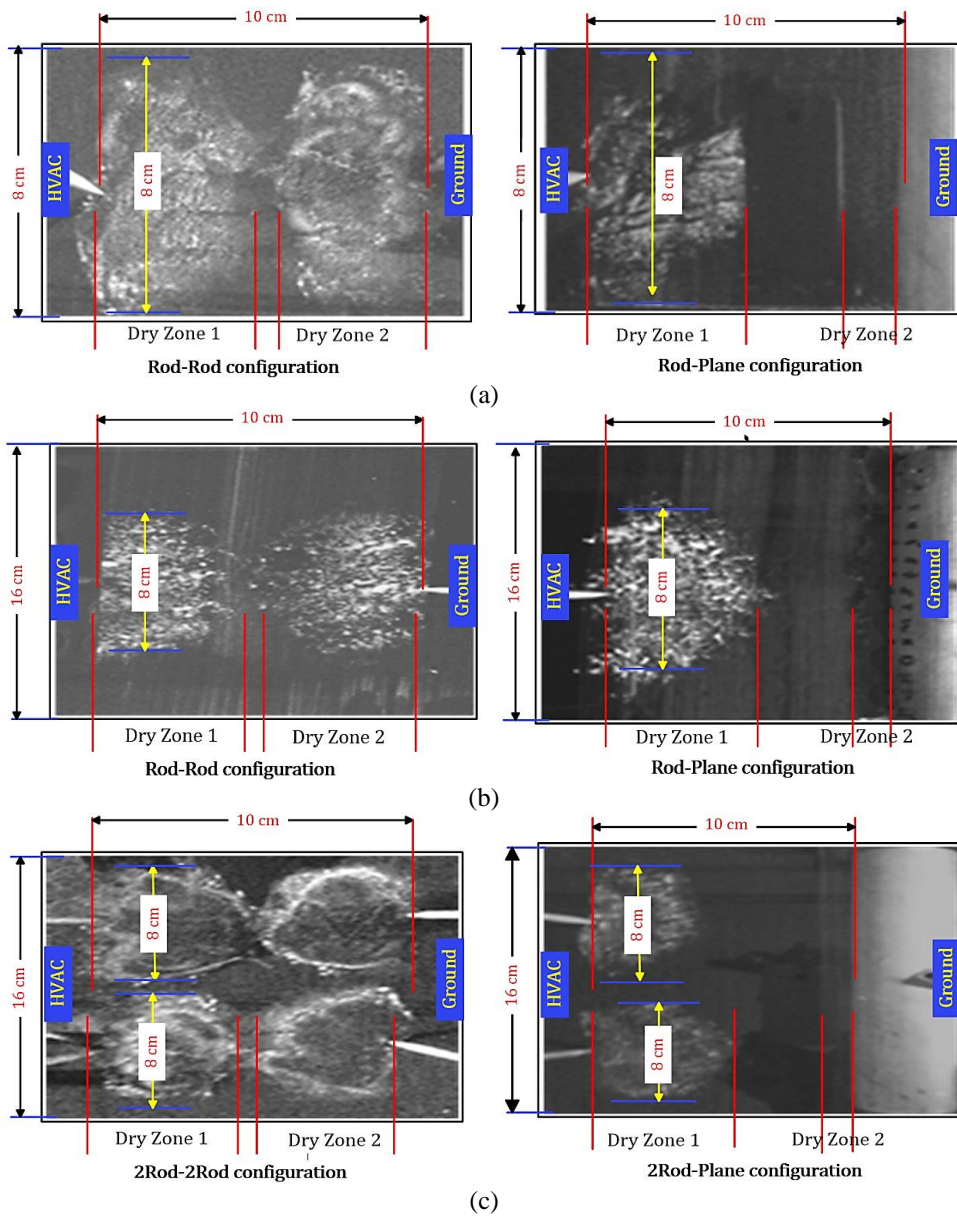


Figure 7. View of the dry band sizes: (a) case of 20×8 cm flat insulator with only one electrode system, (b) case of 20×16 cm flat insulator with only one electrode system, and (c) case of 20×16 cm flat insulator with two electrode system

3.4. Effect of the electrode system configuration

Flashover voltage variation with polluted width L for the glass flat insulator can be clearly seen in Figure 8. The figure shows two families of three curves representing the sample for rod-rod, rod-plane and plane-plane configurations. The conductivity was equal to 0.017 mS/cm and 10 mS/cm respectively.

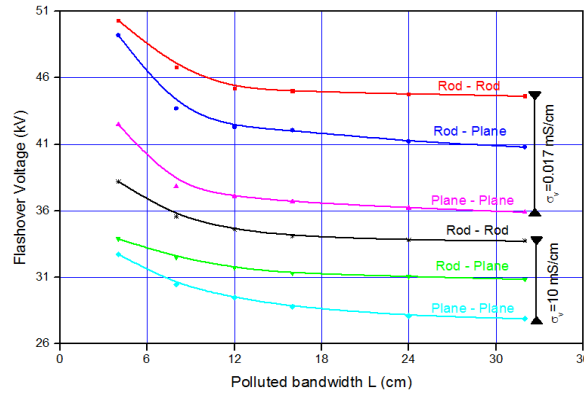


Figure 8. $V_{FO} = f(L)$ Characteristic for different electrode configurations

3.5. Electric equivalence between the plane-plane and multi-rods-rods systems

Figure 9 shows the plot of contamination flashover voltage for different systems of electrodes. This parameter is plotted as a function of the pollution layer's width. As can be seen from Figure 9, contamination flashover voltage is fastly falling with the polluted bandwidth up to a width of around 8 cm. Above 8 cm, a flattening trend of contamination flashover voltage with increase in polluted bandwidth can be seen.

Comparing the different plots, it can be said that they exhibit a similar trend in Figure 9(a). The test results indicate that the change in electrode system configuration does not have any significant effect on the effective width of the electric discharge. They also indicate that the increase of number of rods in Figure 9(b) will tend to decrease the gap in the flashover voltage between the two electrode system configurations.

These tests also reveal that in Figure 10 the number of rods added to the system, with two basic electrodes for example, does not influence the number of parallel electric discharges evolving independently until the ultimate phase of the insulation's flashover. However it does influence the distance separating the two adjacent rods so that the initiation rods of the two parallel discharges are spaced by a distance equal to the effective width. Indeed, the width of 8 cm produces a single arc in Figure 11(a), width of 16 cm produces 02 arcs in Figure 11(b), width of 24 cm produces 03 arcs in Figure 11(c) and the width of 32 cm produces 04 arcs as shown in Figure 11(d). These observations lead us to say that there is an electric equivalence between the multi-rods-rods and plane-plane systems and that the length of 8 cm is a limit above which an arc occurs.

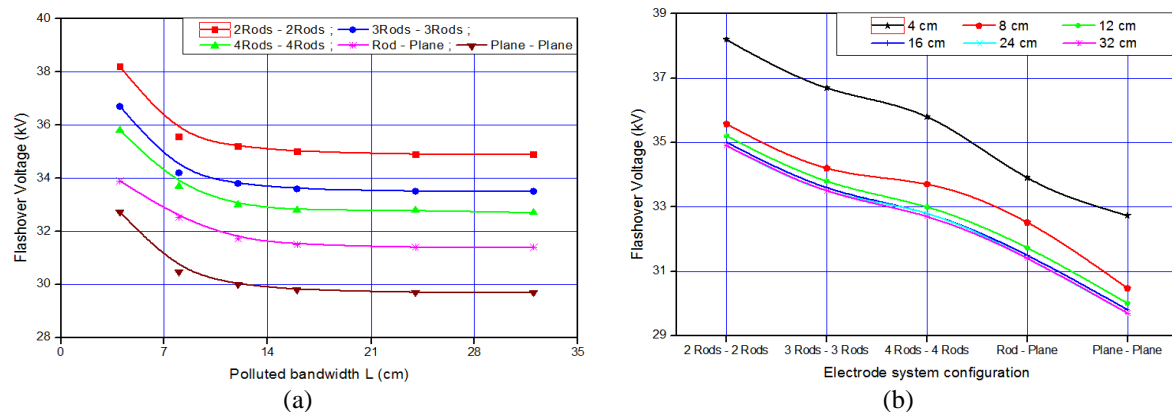


Figure 9. Flashover voltage variation for different rod configurations (a) polluted band width and (b) electrode system configuration

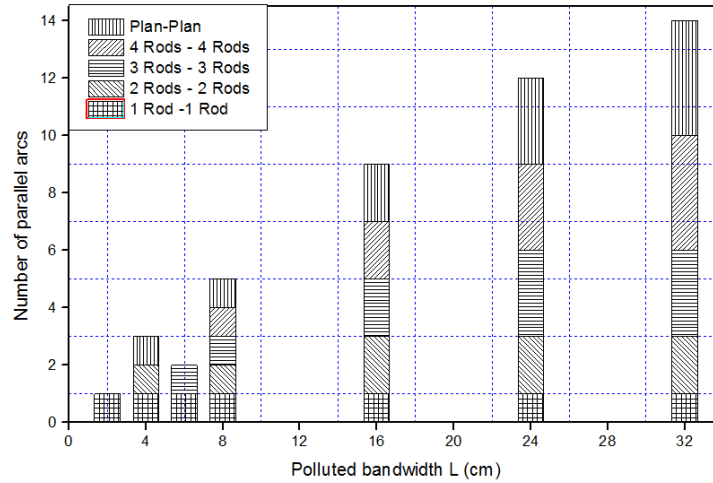


Figure 10. Number of parallel arcs as a function of a polluted bandwidth

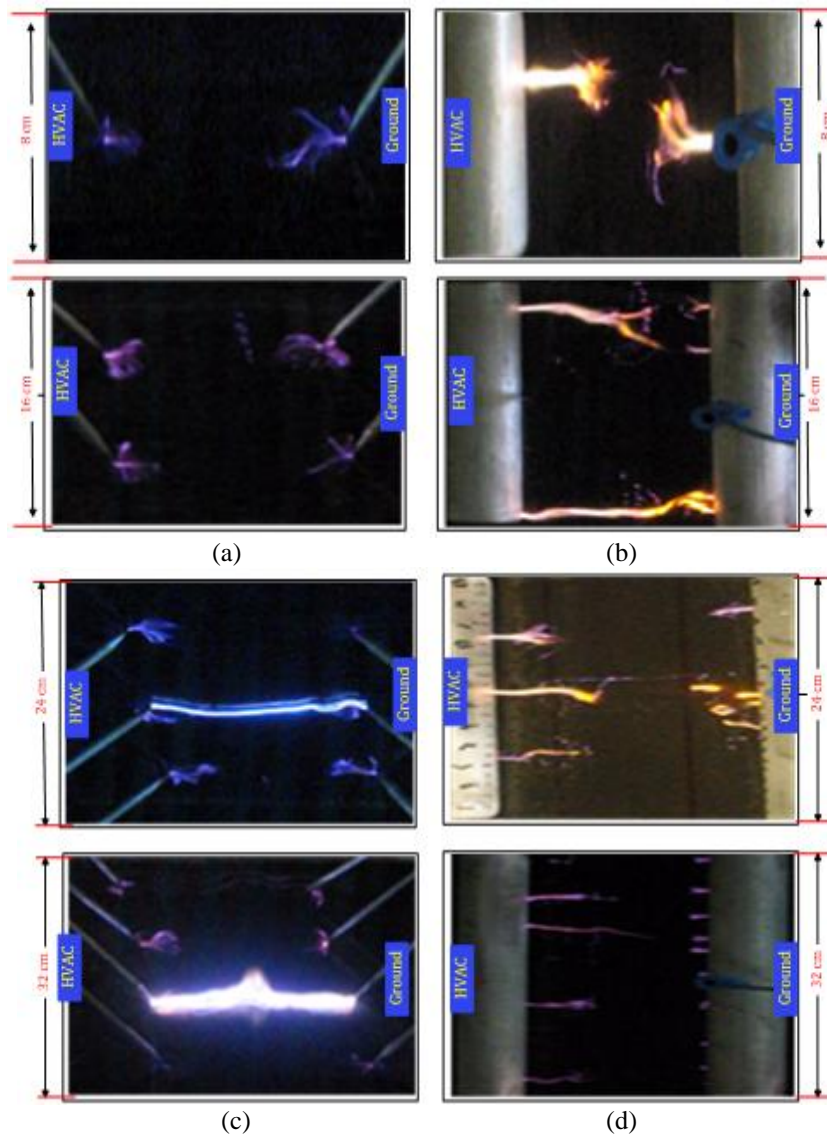


Figure 11. Electric equivalence between the plane-plane and multi-rods-rods systems: (a) 8 cm, (b) 16 cm, (c) 24 cm, and (d) 32 cm

4. CONCLUSION

In this work, extensive tests were carried out characterizing the effective width of partial parallel electric discharges evolving independently on a large insulating surface under AC voltage. Tests were performed under artificial pollution conditions based on the solid layer method of IEC 60507 taking into account the influence of several parameters such as the polluted width, the length of the leakage path, the conductivity and the electrode system configurations. From the data collected from tests presented in this work, it can be concluded that the insulator periphery plays a significant role in contributing to the development of discharges on its surface and greatly affect the flashover voltage and the number of parallel arcs. Therefore, it will dictate the insulator flashover performance. These results showed that only a single electric arc propagates until flashover for small insulator when contaminated uniformly. However, several parallel partial arcs were observed for large insulators. These arcs grow to feed a single arc and may develop to a full flashover. Laboratory tests revealed that an effective width is necessary for a partial discharge to occur. This value is approximately equal to 8 cm. This limit corresponds to the minimal electrical performance of the insulation. Therefore, it can be concluded that the insulators with small diameter exhibit higher flashover voltage values than those with large diameters. At the same time analysis of video recorded during the tests showed equivalence between plane-plane configuration and multi-rod-rod electrode system. Finally, the number of parallel arcs closely depends on the effective width.

ACKNOWLEDGEMENTS

This work is a part of a research project approved under the number: A01L07UN190120180003. The authors would like to thank the Ministry of higher Education and Science Research of Algeria for the financial support of this project.




REFERENCES

- [1] J. S. T. Looms, *Insulators for high voltages*. Institution of Engineering and Technology, 1988.
- [2] F. J. Liprot, "An examination of the service performance of ceramic insulators," in *IEE Colloquium: A Review of Outdoor Insulation Materials*, 1996, vol. 1996, doi: 10.1049/ic:19960039.
- [3] A. Mishra, R. Gorur, and S. Venkataraman, "Evaluation of porcelain and toughened glass suspension insulators removed from service," *IEEE Transactions on Dielectrics and Electrical Insulation*, vol. 15, no. 2, pp. 467–475, Apr. 2008, doi: 10.1109/TDEI.2008.4483466.
- [4] P. J. Lambeth, "Effect of pollution on high-voltage outdoor insulators," *Proceedings of the Institution of Electrical Engineers*, vol. 118, no. 9R, pp. 1107–1130, 1971, doi: 10.1049/piee.1971.0245.
- [5] E. C. Salthouse, "Initiation of dry bands on polluted insulation," *Proceedings of the Institution of Electrical Engineers*, vol. 115, no. 11, pp. 1707–1712, 1968, doi: 10.1049/piee.1968.0298.
- [6] B. F. Hampton, "Flashover mechanism of polluted insulation," *Electronics and Power*, vol. 10, no. 4, 1964, doi: 10.1049/ep.1964.0112.
- [7] F. Obenaus, "Fremdschichtüberschlag und Kriechweglänge," *Deutsche, Electrotechnik*, vol. 4, pp. 135–136, 1958.
- [8] R. Wilkins, "Flashover voltage of high-voltage insulators with uniform surface-pollution films," *Proceedings of the Institution of Electrical Engineers*, vol. 116, no. 3, pp. 457–465, 1969, doi: 10.1049/piee.1969.0093.
- [9] P. Claverie, "Predetermination of the Behaviour of Polluted Insulators," *IEEE Transactions on Power Apparatus and Systems*, vol. PAS-90, no. 4, pp. 1902–1908, Jul. 1971, doi: 10.1109/TPAS.1971.293185.
- [10] F. A. M. Rizk, "Mathematical models for pollution flashover," *Electra*, vol. 78, pp. 71–103, 1981.
- [11] F. Erler, "Zum kriechüberschlag dicker isolatoren bei wechselfeldspannung," *Elektrie*, vol. 23, no. 3, pp. 100–102, 1969.
- [12] M. Khatib, "Influence of diameter on the flashover of polluted overhead line insulators under alternating voltage," Ph.D. thesis, University of Dresden, Germany, 1989.
- [13] H. Matsuo, T. Yamashita, and T. Fujishima, "Shape of contacting surface between an electrolytic solution and local discharge on it," *IEEE Transactions on Dielectrics and Electrical Insulation*, vol. 10, no. 4, pp. 634–640, Aug. 2003, doi: 10.1109/TDEI.2003.1219648.
- [14] R. Boudissa, S. Djafri, A. Haddad, R. Belaicha, and R. Bearsch, "Effect of insulator shape on surface discharges and flashover under polluted conditions," *IEEE Transactions on Dielectrics and Electrical Insulation*, vol. 12, no. 3, pp. 429–437, Jun. 2005, doi: 10.1109/TDEI.2005.1453447.
- [15] S. Flazi, A. Ouis, M. Hamouda, and H. Hadi, "Dynamic features of DC flashover on polluted insulators," *IET Generation, Transmission & Distribution*, vol. 1, no. 1, pp. 8–12, 2007, doi: 10.1049/iet-gtd:20050194.
- [16] Fuzeng Zhang *et al.*, "Experimental investigation on flashover performance of glass insulator for DC transmission lines at high altitudes," in *2007 Annual Report - Conference on Electrical Insulation and Dielectric Phenomena*, 2007, pp. 324–328, doi: 10.1109/CEIDP.2007.4451567.
- [17] M. E.-A. Slama, A. Beroual, and H. Hadi, "Influence of the linear non-uniformity of pollution layer on the insulator flashover under impulse voltage - estimation of the effective pollution thickness," *IEEE Transactions on Dielectrics and Electrical Insulation*, vol. 18, no. 2, pp. 384–392, Apr. 2011, doi: 10.1109/TDEI.2011.5739441.
- [18] A. Mekhaldi, D. Namane, S. Bouazabia, and A. Beroual, "Flashover of discontinuous pollution layer on HV insulators," *IEEE Transactions on Dielectrics and Electrical Insulation*, vol. 6, no. 6, pp. 900–906, 1999, doi: 10.1109/94.822035.
- [19] Z. Zhang, X. Jiang, Y. Chao, L. Chen, C. Sun, and J. Hu, "Study on DC pollution flashover performance of various types of long string insulators under low atmospheric pressure conditions," *IEEE Transactions on Power Delivery*, vol. 25, no. 4, pp. 2132–2142, Oct. 2010, doi: 10.1109/TPWRD.2010.2049132.
- [20] M. E.-A. Slama, A. Beroual, and H. Hadi, "Influence of pollution constituents on DC flashover of high voltage insulators," *IEEE*




- Transactions on Dielectrics and Electrical Insulation*, vol. 20, no. 2, pp. 401–408, Apr. 2013, doi: 10.1109/TDEI.2013.6508740.
- [21] R. Boudissa, A. Bayadi, and R. Baersch, “Effect of pollution distribution class on insulators flashover under AC voltage,” *Electric Power Systems Research*, vol. 104, pp. 176–182, Nov. 2013, doi: 10.1016/j.epsr.2013.06.009.
- [22] N. Bouatia, N. Benouaret, and R. Boudissa, “Research of the equivalence of electrical performance between two plane-plane and point-point configurations with two polluted barriers under alternating current,” (in French), Master thesis, Université Abderrahmane Mira-Bejaia, 2016.
- [23] S. Allali, Y. Nakes, and T. Guia, “Study of high voltage insulator’s flashover,” (in French), Master thesis, Université Echahid Hamma Lakhdar, El-Oued, 2019.
- [24] N. Merzougui and H. Merzougui, “Diagnosis of the surface condition of a high voltage insulator using (current flow problem),” (in French), Master thesis, Université Mohamed Boudiaf, M’sila, 2019.
- [25] N. Ouchenir and S. Remmache, “Study of the inclination angle of the water drop of on the hydrophobicity of a silicone plate aged surface under alternating voltage,” (in French), Master thesis, Université A. Mira-Bejaia, 2019.
- [26] F. Bouchelga and R. Boudissa, “Effect of the development of electrical parallel discharges on performance of polluted insulators under DC voltage,” *IEEE Transactions on Dielectrics and Electrical Insulation*, vol. 22, no. 4, pp. 2224–2233, Aug. 2015, doi: 10.1109/TDEI.2015.005068.

BIOGRAPHIES OF AUTHORS






Samia Satta    was born in Setif, Algeria, in 1982. She obtained the degree of Ingénieur d’Etat in electrical engineering in 2006, the degree of magister in electrical engineering in 2010 from the Electrotechnics Institute of Setif. She is now a PHD student studying the pollution effects on transmission line insulation. She has authored and co-authored more than 15 papers. Email: sattasamia@yahoo.fr.



Abdelhafid Bayadi    obtained the degree of Ingénieur d’Etat in electrical engineering in 1991, the degree of magister in electrical engineering in 1996 from the Electrotechnics Institute of Setif. He joined the same institute in 1998 as an Assistant Professor. He obtained then a Ph.D. degree in high voltage engineering in 2005. In the same year, he was appointed a Senior Lecturer and in 2010, a Professor in electrical engineering at Setif University. His research interests are in power system modelling and simulation, power system transients, high voltage engineering, insulation systems, and power system overvoltage protection. He has co-authored over 150 publications. He is a member of the Steering Committee of the National Conference on High voltage (CNHT). Email: a_bayadi@univ-setif.dz.



Rabah Boudissa    obtained a degree in electrical engineering from the Polytechnic National School of Algiers in 1982 and in 1992 he obtained the Ph.D. degree in high voltage engineering from T. H. Zittau, Germany. In 1983, he was appointed a lecturer in High Voltage Engineering and Materials at both undergraduate and post-graduate levels at the University of Bejaia, Algeria, and in 2013, Professor in electrical engineering at same University. In 2014 he was the director of research of the Laboratory of Electric Engineering of Bejaia (LGEB). He trains masters and doctorates in specialty of high voltage and electrical networks. His main research interests are the effects of pollution and lightning on power systems and equipments. He has co-authored over 100 publications. He is a member of the Steering Committee of the National Conference on High voltage (CNHT). <https://www.researchgate.net/profile/Rabah-Boudissa>, Prof; Rabah Boudissa passed away on 25/08/2021 at an age of about 64 years. Email: raboudissa@yahoo.fr.